

In vitro bioactivity of 3D Ti-mesh with bioceramic coatings in simulated body fluid



Wei Yi ^a, Xudong Sun ^a, Dun Niu ^{b,*}, Xiaozhi Hu ^{c,**}

^a Key Laboratory for Anisotropy and Texture of Materials (Ministry of Education), Northeastern University, Shenyang 110819, China

^b School of Science, Northeastern University, Shenyang 110819, China

^c School of Mechanical and Chemical Engineering, The University of Western Australia, Perth 6009, Australia

ARTICLE INFO

Article history:

Received 6 January 2014

Received in revised form 8 April 2014

Accepted 8 April 2014

Available online 29 April 2014

Keywords:

Hydroxyapatite

Bioglass

Bioactivity

Simulated body fluid

Apatite

ABSTRACT

3D Ti-mesh has been coated with bioceramics under different coating conditions, such as material compositions and micro-porosity, using a dip casting method. Hydroxyapatite (HA), micro-HA particles (HAp), a bioglass (BG) and their different mixtures together with polymer additives were used to control HA-coating microstructures. Layered composites with the following coating-to-substrate designs, such as BG/Ti, HA + BG/BG/Ti and HAp + BG/BG/Ti, were fabricated. The bioactivity of these coated composites and the uncoated Ti-mesh substrate was then investigated in a simulated body fluid (SBF). The Ti-mesh substrate and BG/Ti composite did not induce biomimetic apatite deposition when they were immersed in SBF for the selected BG, a pressable dental ceramic, used in this study. After seven days in SBF, an apatite layer was formed on both HA + BG/BG/Ti and HAp + BG/BG/Ti composites. The difference is the apatite layer on the HAp + BG/BG/Ti composite was rougher and contained more micro-pores, while the apatite layer on the HA + BG/BG/Ti composite was dense and smooth. The formation of biomimetic apatite, being more bioresorbable, is favored for bone regeneration.

© 2014 The Ceramic Society of Japan and the Korean Ceramic Society. Production and hosting by Elsevier B.V. All rights reserved.

1. Introduction

Titanium (Ti) has been widely used to make dental and orthopedic implants [1] due to its excellent mechanical properties and chemical stability in the human body environment [2]. Unfortunately, stress shielding occurs when a fixation device, e.g. a solid bulk Ti implant, has an elastic modulus substantially higher than that of the surrounding bone tissue. The modulus of Ti is higher than that of the natural bone, and Ti does not promote bone tissue regeneration [3]. It is known that bioceramics such as hydroxyapatite (HA) [4], and bioglass (BG) [5] are bioresorbable and able to bond with living bone through bone regeneration, and have therefore been tested clinically as bone substitutes [6]. However, applications

of these bioceramics are restricted to non-load bearing implants due to their poor flexural strength and fracture toughness [7,8]. It appears that Ti and bioceramic composites would be better options to combine the strength and reliability of Ti and bio-properties of those resorbable bioceramics.

Bioceramic-coated Ti composites have been developed by using various coating techniques, such as the plasma spray [9–11] and sol-gel [12,13] techniques. Bioceramic coatings deposited by these techniques are normally thin (e.g. limited to a few hundred microns) and dense.

In our previous study [14], we tried a simple multi-layered dip casting method in order to increase the HA coating thickness and create micro-porous coating structures around 3D Ti-mesh. The effective modulus of a HA-coated 3D Ti-mesh (or Ti-mesh reinforced HA scaffold) is much less than that of bulk solid Ti, and the composite has the attractive bio-properties of HA. The key aspect of the process is the use of a BG layer to join the micro-porous HA-coating to a dense Ti-mesh.

In this study, we investigated the in vitro bioactivity of the bioceramic-coated Ti-mesh composites under different coating conditions, such as BG coating, HA-BG coating, and HAp (HA particles)-BG coating. HAp is introduced as a means of changing the coating porosity. Since a bone implant will immediately come in contact with body fluids during surgery, far before bone tissue regeneration, it is useful to examine the reactions between simulated body fluid (SBF) and various bioceramic coatings.

* Corresponding author. Tel.: +86 24 8368 4533; fax: +86 24 8368 4533.

** Corresponding author. Tel.: +61 8 6488 2812; fax: +61 8 6488 1024.

E-mail addresses: xyz6527753@163.com (D. Niu),

xiao.zhi.hu@uwa.edu.au (X. Hu).

Peer review under responsibility of The Ceramic Society of Japan and the Korean Ceramic Society.



Production and hosting by Elsevier

It has been accepted that one essential requirement for an artificial biomaterial to exhibit a bone bonding to living bone is the formation of a bone-like apatite layer on its surface in body environment [15]. In fact, the presence of a bone-like apatite layer on the surface of an orthopedic biomaterial is considered as a positive biological response from the host tissue [16]. Previous studies have proven that SBF, which contains ion concentrations approximately equal to those in human blood plasma (HBP) and was first used by Kokubo et al. [17], can well reproduce the *in vivo* surface changes in certain biomaterials [18]. So investigating the biological behavior of biomaterials in the SBF is considered the most efficient and economical way to test their bioactivity in the body environment.

2. Experimental

2.1. Materials

A commercially pure (cp) Ti-mesh for surgical applications (Grade 2, Baoji INT Titanium Materials Co. Ltd., Baoji, China) was selected as the Ti substrate in the present study. HA (around 30 nm, Beijing DK Nano S&T Ltd., Beijing, China), BG or pressable dental ceramic (9 µm, VITA PM9 Zahnfabrik H. Rauter GmbH KG, Bad Säckingen, Germany) and nano-sized silica (around 10 nm, Sigma-Aldrich, St. Louis, MO, USA) were used as the starting coating materials. Polymethylmethacrylate (PMMA) (Sigma-Aldrich) and starch were used as micro-pore forming agents. Polyvinylalcohol (PVA) and glycerol were used as binders. More details on the raw materials could be found in our previous study [14].

2.2. Specimen processing

HA particles (HAp, about 75 µm) were fabricated from the starting HA by a pre-sintering and milling process. HA powder was pressed in a steel mold, and then the green body was pre-sintered at 700 °C for 2 h in a muffle furnace. Micro-HA particles, Hap, were produced by crushing the pre-sintered HA sample, followed by sieving to the desired size range.

Three different slurries were prepared by mixing different reagents, which were used to coat different bioceramic layers on the Ti-mesh substrate. Slurry A (for bonding on Ti) was prepared by mixing 20 vol% of BG, 5 vol% silica, and in total 15 vol% of PVA, glycerol and starch in 60 vol% of distilled water and ethanol mix. Slurry B (micro-porous HA coating of the outer surface) was prepared by mixing 20 vol% of HA, 5 vol% of BG, and in total 15 vol% of PVA, glycerol and starch, 10 vol% of PMMA micro-particles up to 50 µm in diameter in 50 vol% of distilled water and ethanol mix. Slurry C (micro-porous HA coating of the outer surface) was prepared by mixing 20 vol% of HAp, 5 vol% of BG, and in total 15 vol% of PVA, glycerol and starch, 10 vol% of PMMA micro-particles up to 50 µm in diameter in 50 vol% of distilled water and ethanol mix. These slurries were ball-milled for 4 h before being used for the dip casting. Different 3D Ti-mesh samples were dipped into slurry A, then taken out and left for drying; this process was repeated to ensure complete 3D coating. Subsequently, the samples were sintered at 700 °C for 1 min in vacuum and cooled down slowly to the room temperature. At this stage, the BG/Ti composite was prepared.

The BG/Ti composite samples were dipped into slurry B and slurry C, respectively, then taken out and left for drying. Again, the process was repeated to obtain thicker coatings. These samples were sintered at 900 °C for 10 min in a muffle furnace and cooled down to the room temperature. Finally, the HA + BG/BG/Ti composite and the HAp + BG/BG/Ti composite were fabricated. Nano-sized HA starting powders and BG helped to lower the sintering temperature of HA coating, which was set at 900 °C to minimize oxidation of the Ti-mesh.

2.3. SBF immersion

After the as-fabricated composite and Ti substrate were washed ultrasonically in acetone and deionized water, and dried in oven, an *in vitro* bone-like layer growth test was performed by soaking the samples (sample size approx. 23.5 mm²) at 36.5 °C in 30 ml of SBF in polyethylene bottles for 7 days with stirring but without refreshing the solution. The chemical compositions and pH of SBF vs. HBP are listed in Table 1. The detailed preparation of SBF adopted in this study followed the work of Kokubo and Takadama [18].

2.4. Phase composition and microstructure characterization

X-ray diffraction (XRD) (Empyrean, PANalytical, the Netherlands, CuK α radiation at 40 kV) was performed to analyze the phases in the composite coating surface. Micro-structures of the as-fabricated composite and Ti substrate were observed by Field Emission Scanning Electron Microscopy (Zeiss 55, Jena, Germany). The phases and features of the bone-like layer formed on the composite surfaces after SBF immersion were carefully examined by the XRD and FESEM incorporating X-ray microanalysis using energy dispersive spectrometry (EDS).

3. Results and discussion

3.1. Surface microstructures of Ti substrate and as-sintered composite before and after SBF tests

Microstructures of the Ti substrate and BG/Ti composite before and after SBF treatment are shown in Fig. 1. The original Ti-grid surface in Fig. 1(a) is very similar to that of the same Ti-substrate after 7 days in SBF shown in Fig. 1(b). Similarly, the original surface of the BG-coated Ti-grid surface in Fig. 1(c) is virtually identical to that of the BG/Ti composite after 7 days in SBF. Therefore, biomimetic apatite crystal formation or deposition on both Ti and BG surfaces is negligible, if it ever occurred.

While the specific BG, selected primarily to seal the Ti substrate in this study, is not bioactive by itself, the overall bioactivity of the BG/Ti composite can be enhanced by incorporating bioactive HA powders and pre-sintered micro-HAp into the BG coating. Indeed, the surface features of both HA + BG/BG/Ti and HAp + BG/BG/Ti composites changed after 7 days in SBF because of deposition of biomimetic apatite crystals.

The surface microstructure of the HA + BG/BG/Ti composite is shown in Fig. 2(a). Here (HA + BG) implies that the top coating

Table 1
Ion concentrations and pH in SBF solution and HBP.

Fluid	Contents (mM except for pH)								
	Na ⁺	K ⁺	Mg ²⁺	Ca ²⁺	Cl ⁻	HCO ₃ ²⁻	HPO ₄ ²⁻	SO ₄ ²⁻	
SBF	142.0	5.0	1.5	2.5	148.8	4.2	1.0	0.5	7.40
HBP	142.0	5.0	1.5	2.5	103.0	27.0	1.0	0.5	7.35–7.45

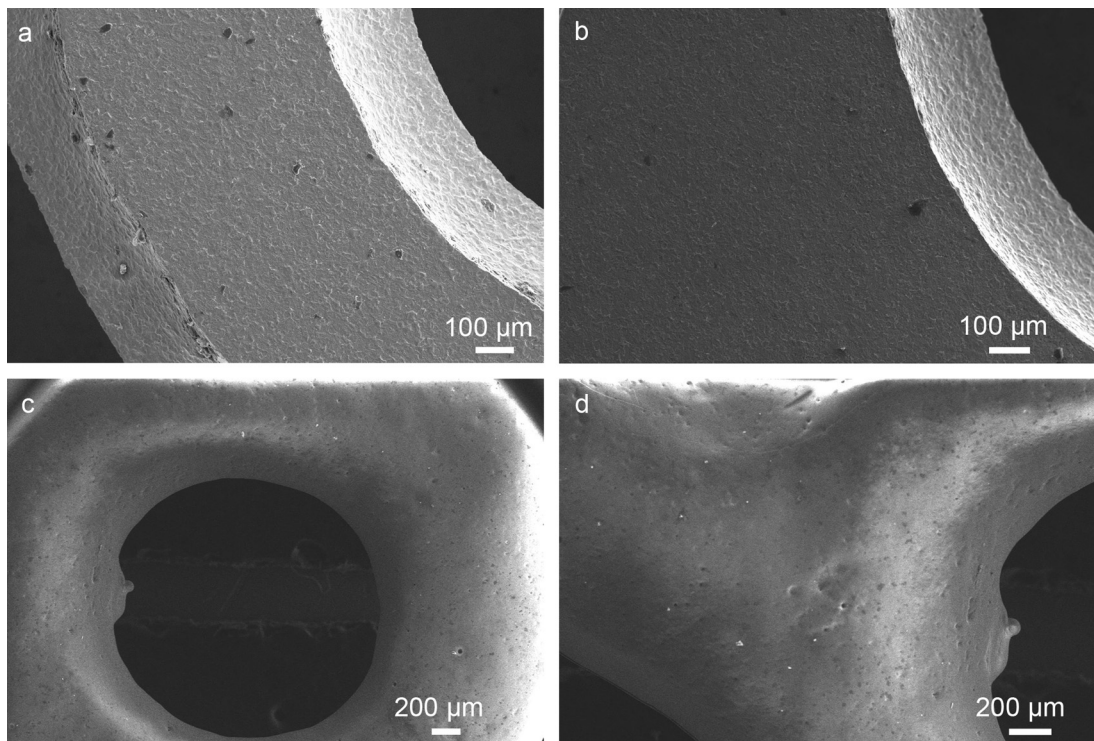


Fig. 1. The surface features of Ti-mesh substrate and BG/Ti composite before and after 7 days in SBF: (a) original Ti substrate; (b) Ti substrate after 7 days in SBF; (c) original BG/Ti composite; and (d) BG/Ti composite after 7 days in SBF.

contains both HA powder and BG, and thus it is possible that HA may not cover the entire outer surface after sintering. This has been confirmed in Fig. 2(a), where the rounded smooth areas are BG regions. Interestingly, after 7 days in SBF, the same surface with

both HA and BG was completely covered by a dense and regular apatite crystal coating as shown in Fig. 2(b). This proves that apatite crystal deposition first occurs at the HA sites and then spreads out over the entire surface.

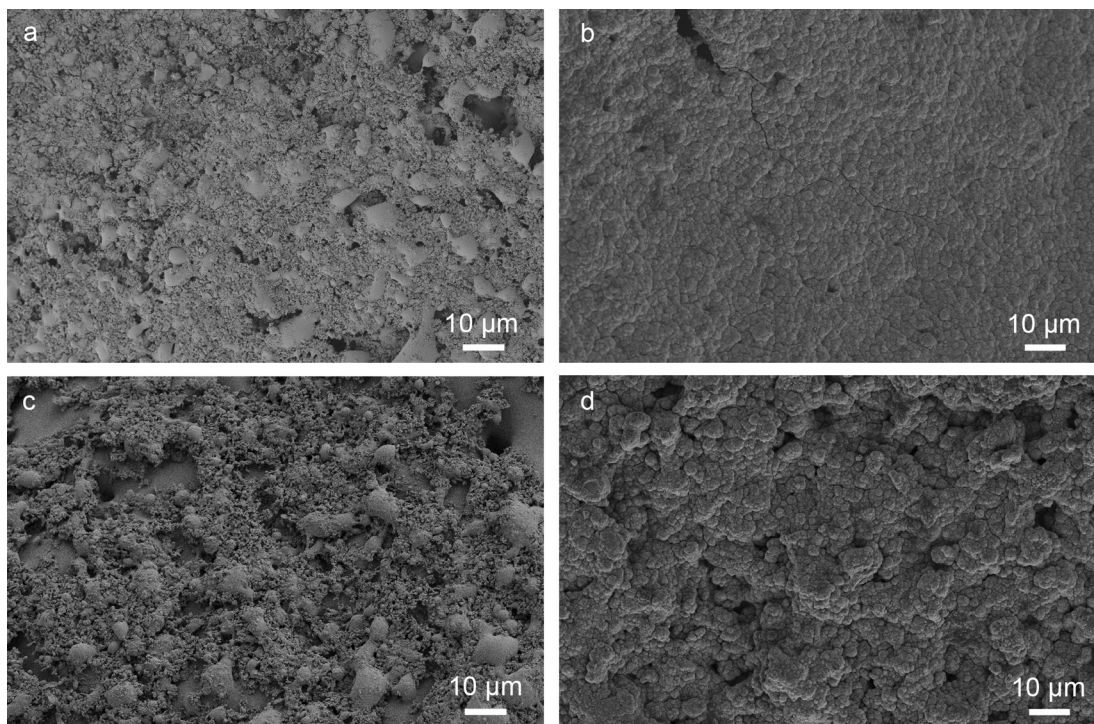


Fig. 2. The surface features of the HA + BG/BG/Ti and HAp + BG/BG/Ti composites before and after 7 days in SBF: (a) original HA + BG/BG/Ti composite; (b) HA + BG/BG/Ti composite after 7 days in SBF; (c) original HAp + BG/BG/Ti composite; and (d) HAp + BG/BG/Ti composite after 7 days in SBF, i.e. HAp is associated with coarser apatite grain formations and rougher coating surface.

The surface microstructure of the HA_p + BG/BG/Ti composite is much rougher when pre-sintered micro-HA particles (instead of HA powders) were embedded in the top (HA_p + BG) coating, as can be seen in Fig. 2(c). In fact, the purpose of using HA_p particles instead of as-received HA powders is to modify the top coating microstructures and porosity. Once again, after 7 days in SBF, the HA_p + BG/BG/Ti composite is fully covered by the biomimetic apatite crystal layer with a rougher surface finish, as in Fig. 2(d).

The size of micro-HA_p can be varied to alter the “roughness” of the apatite-crystal coating and its micro-pore structures, which can be useful in osseointegration during bone healing. While the polymer additives and HA_p were used to create micro-pores or openings (around 10 μm or less) in the HA coatings, larger open pores (>100 μm) suitable for bone ingrowth can be generated using a recently developed HA-coating technique based on dip casting and freeze-drying [19]. However, if 3D Ti-mesh structures (with opening over 600–1000 μm) are considered as Ti-scaffolds, HA coatings (with micro-pores <10 μm) on the Ti-mesh may be adequate for bone ingrowth. The 3D composite can be considered either as a Ti-mesh reinforced HA-scaffold or as a HA-coated Ti-scaffold.

3.2. The phase compositions of apatite-crystal coatings

The XRD patterns of the HA + BG/BG/Ti composite before and after 7 days in SBF are shown in Fig. 3. The as-sintered HA + BG/BG/Ti composite in Fig. 3(b) shows peaks of HA, feldspar and leucite,

indicating that the surface contains both BG (with bi-phase feldspar and leucite) and HA. As there is no Ti peak in Fig. 3(b), the two-layer HA + BG/BG coatings have completely covered the Ti substrate.

After 7 days in SBF, only HA peaks can be detected over the HA + BG/BG/Ti composite, as in Fig. 3(a), indicating that the biomimetic apatite crystals have completely covered the composite surface. These naturally formed apatite crystals are more bioactive and more bioresorbable, and thus can potentially lead to faster bone healing and regeneration.

An overview and an enlarged surface section of the HA + BG/BG/Ti composite are shown in Fig. 4. While the overview in Fig. 4(a) only displays the uneven distributions of sintered HA, exposed BG and micro-pores, the enlarged section in Fig. 4(b) shows interesting details on the HA formations over the BG matrix. The HA clusters varying from 1 to 5 μm are micro-porous, with uniform micro-pores far less than 500 nm. The formation of HA clusters by sintering of HA powders and BG and the associated rough surface finish suggest that the micro-open-pore structures in the HA–BG coating and its roughness can be effectively tailored by incorporating pre-sintered HA_p of different sizes. The smooth BG region in Fig. 4(b) appears to be covered by uniform tiny black dots. They are not isolated HA powders, but isolated leucite phases in the continuous feldspar matrix [20].

Surface microstructures of the HA + BG/BG/Ti biocomposite after 7 days in SBF are shown in Fig. 5 with different magnifications. The EDS analysis of the apatite-crystal coating compositions is also displayed. The apatite-coating surface in Fig. 5(a) with a low magnification appears to be dense and smooth, which also appears to have regular “grain” structures. Fig. 5(c) with a higher

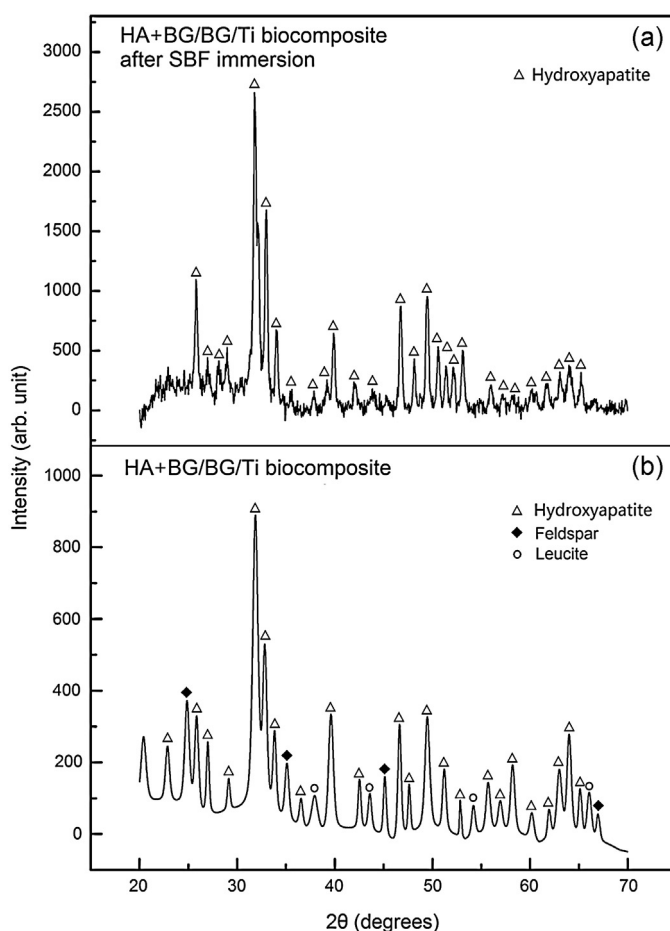


Fig. 3. XRD patterns: (a) apatite-crystal coating over HA + BG/BG/Ti composite, showing only HA peaks, after 7 days in SBF and (b) original as-sintered HA + BG/BG/Ti composite showing the presence of BG.

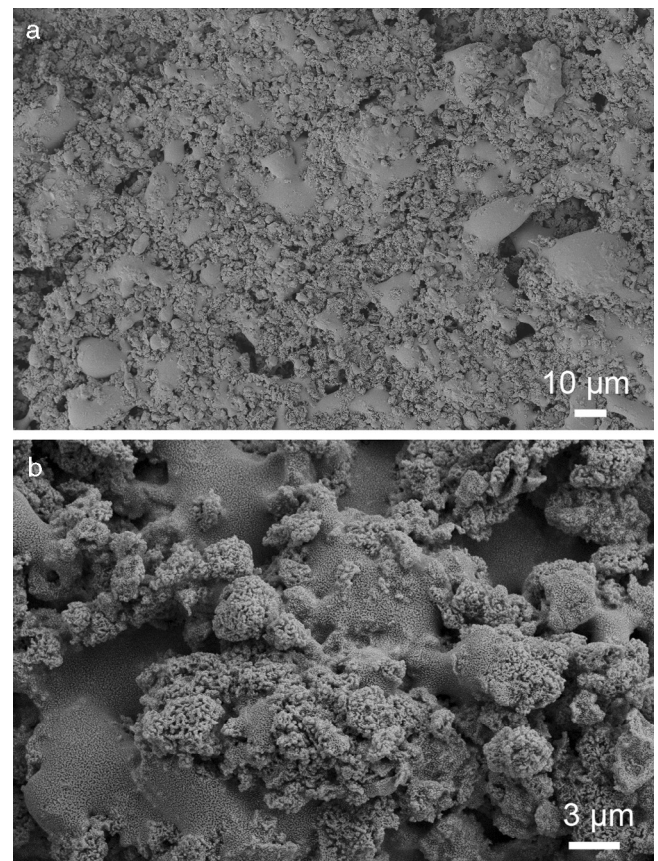


Fig. 4. The surface features of HA + BG/BG/Ti composite: (a) as-sintered surface with agglomerated HA regions joined by BG and (b) close-up of (a) showing sintered HA-clusters distributed within the BG matrix.

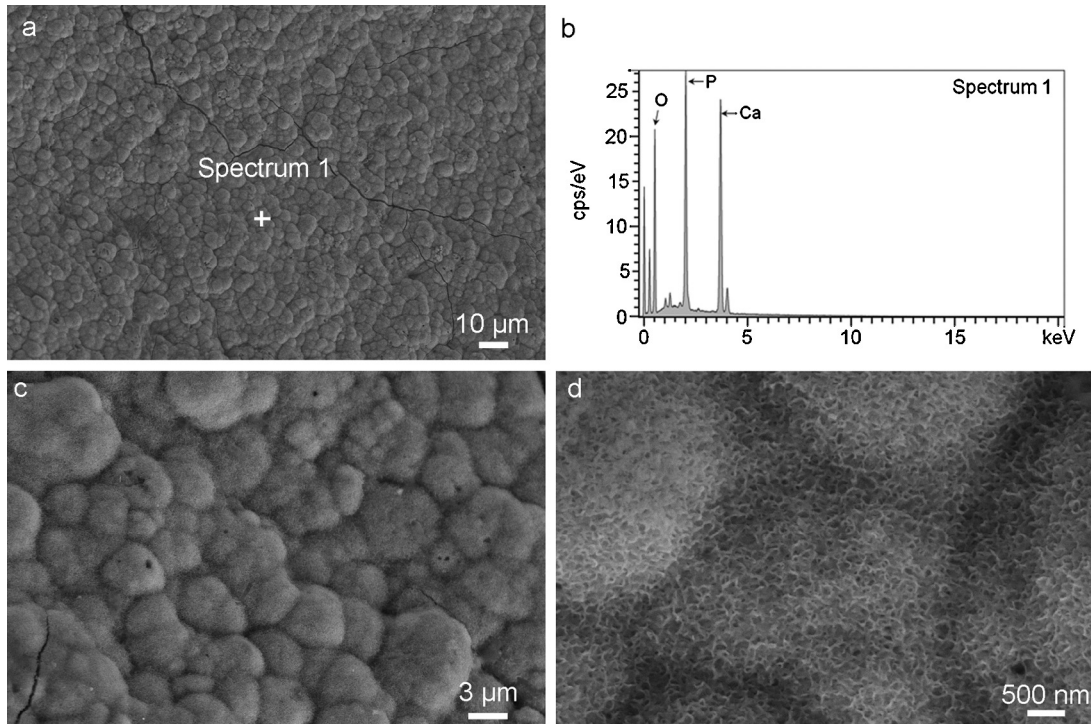


Fig. 5. The microstructure of the HA+BG/BG/Ti biocomposite surface after 7 days in SBF: (a) typical “dense” surface features of the apatite formation; (b) EDS analysis at the marked surface location in (a); (c) close-up from (a) showing “fluffy” crystal surface; and (d) higher magnification showing “grass-like” apatite nano-crystals.

magnification shows that these “grains” do not have smooth, but fluffy surfaces. Fig. 5(d) with an even higher magnification shows that each “grain” is formed by nano-sized apatite formations. Similar microstructures were reported previously in the literatures [21–23].

The XRD patterns in Fig. 3(a) and the EDS analysis in Fig. 5(b) confirm the presence of apatite crystal formations deposited on the composite surface in SBF. This is because a typical location in Fig. 5(a), Spectrum 1 (or Location 1), shows clearly Ca, P and O peaks, while in Fig. 5(b) other peak signals are very weak. According to the XRD pattern (Fig. 3(a)), only HA crystal is characterized, so the compound consisting of Ca, P and O at Location 1 is apatite crystal.

4. Conclusions

3D Ti mesh has been successfully coated with HA, BG and their different mixtures, using a dip casting method. The key role of BG is to weld the micro-porous HA-coating to the dense Ti-substrate during the process of sintering. Being not bioresorbable, the BG inner coating can effectively seal out the Ti-mesh to prevent the possible release of micro-Ti-particles to its surrounding environment. Bioresorbable HA and HAp in the surface coating can attract the formation of biomimetic apatite crystals on the outer surface of the composite, making it more natural and more bioresorbable when used as a bone implant.

Our SBF tests show that it is not necessary to coat the entire outer surface with HA or HAp, but seeding of bioactive HA and HAp in the BG matrix is sufficient to induce the biomimetic apatite coating, which can effectively spread over the entire outer surface.

Acknowledgements

This work was supported by the Joint Funds of the National Natural Science Foundation of China (U1302272) and Australian Research Council's Discovery Project Grant (DP110105296). W. Yi

is grateful for financial support by the China Scholarship Council (CSC) (2010608030), and supports at the University of Western Australia (UWA) (10300003) for the experiments. The authors thank the technical assistance of Center for Microscopy, Characterization & Analysis at UWA.

References

- [1] M. Geetha, A.K. Singh, R. Asokamani and A.K. Gogia, *Prog. Mater. Sci.*, **54**, 397–425 (2009).
- [2] L.C. Zhang, D. Klemm, J. Eckert, Y.L. Hao and T.B. Sercombe, *Scr. Mater.*, **65**, 21–24 (2011).
- [3] J.R. Porter, T.T. Ruckh and K.C. Popat, *Biotechnol. Progr.*, **25**, 1539–1560 (2009).
- [4] H.-W. Kim, Y.-H. Koh, L.-H. Li, S. Lee and H.-E. Kim, *Biomaterials*, **25**, 2533–2538 (2004).
- [5] K. Stanton, K. O'Flynn, S. Nakahara, J.-F. Vanhumbeeck, J. Delucca and B. Hooghan, *J. Mater. Sci. Mater. Med.*, **20**, 851–857 (2009).
- [6] L.L. Hench, *J. Am. Ceram. Soc.*, **74**, 1487–1510 (1991).
- [7] C.Q. Ning and Y. Zhou, *Biomaterials*, **25**, 3379–3387 (2004).
- [8] Z.M. Xiu, Y. Liu, J.G. Li, D. Huo, X.D. Li, X.D. Sun, K. Duan and X.Z. Hu, *Adv. Mater. Res.*, **41**, 41–48 (2008).
- [9] Y.C. Tsui, C. Doyle and T.W. Clyne, *Biomaterials*, **19**, 2015–2029 (1998).
- [10] X. Zheng, M. Huang and C. Ding, *Biomaterials*, **21**, 841–849 (2000).
- [11] Y. Yang, K.-H. Kim and J.L. Ong, *Biomaterials*, **26**, 327–337 (2005).
- [12] E. Millella, F. Cosentino, A. Licciulli and C. Massaro, *Biomaterials*, **22**, 1425–1431 (2001).
- [13] H.-W. Kim, H.-E. Kim and J.C. Knowles, *Biomaterials*, **25**, 3351–3358 (2004).
- [14] W. Yi, X.Z. Hu, X. Sun, P. Ichim and A. Suvorova, *Int. J. Appl. Ceram. Technol.*, **10**, 1–9 (2013).
- [15] V. Karageorgiou and D. Kaplan, *Biomaterials*, **26**, 5474–5491 (2005).
- [16] A.C. Jones, C.H. Arns, A.P. Sheppard, D.W. Hutmacher, B.K. Milthorpe and M.A. Knackstedt, *Biomaterials*, **28**, 2491–2504 (2007).
- [17] T. Kokubo, H. Kushitani, S. Sakka, T. Kitsugi and T. Yamamuro, *J. Biomed. Mater. Res.*, **24**, 721–734 (1990).
- [18] T. Kokubo and H. Takadama, *Biomaterials*, **27**, 2907–2915 (2006).
- [19] B. Jiang, X.Z. Hu and Z.H. Huang, *Mater. Lett.*, **109**, 66–69 (2013).
- [20] W. Yi, X.Z. Hu, P. Ichim and X.D. Sun, *J. Am. Ceram. Soc.*, **96**, 3662–3669 (2013).
- [21] J. Huang, S.M. Best, W. Bonfield and T. Buckland, *Acta Biomater.*, **6**, 241–249 (2010).
- [22] I. Demnati, D. Grossin, C. Combes, M. Parco, I. Braceras and C. Rey, *Biomed. Mater.*, **7**, 1–10 (2012).
- [23] H. Maeda, T. Kasuga and L.L. Hench, *Biomaterials*, **27**, 1216–1222 (2006).